

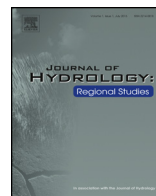


ELSEVIER

Contents lists available at ScienceDirect

## Journal of Hydrology: Regional Studies

journal homepage: [www.elsevier.com/locate/ejrh](http://www.elsevier.com/locate/ejrh)



# Hydrological responses to climate change in Mt. Elgon watersheds



J. Musau<sup>a,b,\*</sup>, J. Sang<sup>a</sup>, J. Gathenya<sup>a</sup>, E. Luedeling<sup>b</sup>

<sup>a</sup> Biomechanical and Environmental Engineering Department, Jomo Kenyatta University of Agriculture and Technology (JKUAT), Kenya

<sup>b</sup> World Agroforestry Centre (ICRAF), Gigiri, Nairobi, Kenya

### ARTICLE INFO

#### Article history:

Received 5 June 2014

Received in revised form 3 December 2014

Accepted 8 December 2014

Available online 12 January 2015

#### Keywords:

Climate change

Streamflow

Nzoia basin

Mt. Elgon

SWAT

### ABSTRACT

**Study Region:** The Upper catchments of the Nzoia River basin in western Kenya.

**Study Focus:** The potential streamflow responses to climate change in the upper Nzoia River basin are studied. The Soil and Water Assessment Tool (SWAT) was forced with monthly temperature and precipitation change scenarios for the periods 2011–2040 (2020s), 2041–2070 (2050s) and 2071–2100 (2080s). Data from 10 climate models and three greenhouse gases emission scenarios was down-scaled using the delta change method and used in the SWAT model. Streamflow data for the periods 1986–1998 and 1973–1985 was used for model calibration and validation respectively.

**New Hydrological Insights for the Region:** Comparison between the simulated baseline and future streamflow shows that in the Koitobos and Kimilili watersheds, August to December streamflow is likely to be highly altered. In the Kuywa watershed, March to June flows is likely to change considerably due to climate change. Major streamflow changes are likely in March to June and August to November in the Rongai watershed. Projected changes differed between the four watersheds despite their proximity, indicating different sensitivities to climate change and uncertainty about the potential hydrological impacts of climate change in the area.

© 2015 The Authors. Published by Elsevier B.V. This is an open access article under the CC BY-NC-ND license (<http://creativecommons.org/licenses/by-nc-nd/4.0/>).

\* Corresponding author at: Biomechanical and Environmental Engineering Department, Jomo Kenyatta University of Agriculture and Technology (JKUAT), Kenya. Tel.: +254 716343094.

E-mail address: [johnkuyega@gmail.com](mailto:johnkuyega@gmail.com) (J. Musau).

## 1. Introduction

Increasing concentrations of atmospheric greenhouse gases (GHGs), and consequent global warming are almost certainly responsible for significant changes in global climatic patterns (IPCC, 2007; Xu et al., 2011). Climate change impacts are most severely experienced by communities whose livelihoods are heavily dependent on climate-sensitive sectors such as agriculture, water resources and forestry (Xu et al., 2013). Shifts in the availability of water resources are expected to be among the most significant consequences of projected climate changes (IPCC, 2007; Kingston and Taylor, 2010). Perturbations to the hydrological system will have implications for runoff volume and timing, ecosystem dynamics, social and economic systems. The intensity of the impacts at local level and the vulnerability of communities and ecosystems to these impacts are highly dependent on the particular characteristics of the area, as well as the magnitude and spatial distribution of the changes that will be experienced (Hagg et al., 2007; Matondo et al., 2004).

Given the vital role of water resources in socio-economic development, the potential hydrological impacts of climate change pose a significant challenge for water resource planning and management. Consequently, such impacts of climate change have been widely studied, mainly using water balance models coupled with General Circulation Models (GCMs). Impacts have been attributed to the associated long-term changes in the dominant climate variables: precipitation and temperature (Chien et al., 2013; Hansen et al., 2006). The hydrological simulations based on climatic projections have shown relatively minor dependence on the hydrological model used compared to the choice of climate models (Bates et al., 2008; Kay et al., 2006). Although GCMs are primary tools for climate change impact assessment, there is a mismatch between the fine-scale nature of local hydrological processes and the coarse resolution of GCMs. Consequently, downscaling techniques varying in complexity and approach have been developed and used (Liu et al., 2008; Murphy, 1998; Wilby and Wigley, 1998; Xu, 1999).

Despite the growing interest in assessing the hydrological impacts of climate change, the underlying uncertainties in simulation of hydrological responses to climate change are still a challenge. Under stable climate conditions and/or physical characteristics, errors in the model structure, calibration procedure, and calibration data are the main sources of uncertainties (Bastola et al., 2011; Brigode et al., 2013; Yang et al., 2008). In non-stationary conditions, such as will occur under climate change, the coarse resolution of the climate models, their representation of the atmospheric and other processes, and differences in results of downscaling techniques are key concerns (Braga et al., 2013; Chiew et al., 2010; Ficklin et al., 2009; Minville et al., 2008; Teng et al., 2012; Xu et al., 2011). Although the relative significance of the different sources of uncertainty has not often been quantified, studies have shown that uncertainties from GCM outputs are more significant than those from hydrological models (Arnell, 2011; Chen et al., 2011; Teng et al., 2012).

In the Nzoia River basin, the target area of this study, historical occurrence of extreme hydrological conditions with dire consequences for local populations have already exposed the vulnerability of human and natural systems to hydrological changes. Land use on the slopes of Mt. Elgon is characterized by conflict between conservation measures and subsistence farming. Frequent landslides and floods initiated by high rainfall and land degradation in the area have claimed lives and destroyed property in the recent past (Claessens et al., 2007). The area is endowed with a rich biodiversity, which influences lives and livelihoods of thousands of people through provision of ecosystem services and products (Petursson et al., 2006). This area forms the upper reaches of the Nzoia River and contributes a significant proportion to its streamflow volume. However, climate change is likely to affect hydrological processes, possibly increasing the vulnerability of farmers to natural variation. Assessment of the potential climate change impacts on streamflow is therefore crucial for disaster preparedness, irrigation planning and structural development. Since the area has not received adequate attention in climate change impact assessment, this study seeks to assess the potential impacts of climate change on streamflow in Mt. Elgon watersheds using the Soil and Water Assessment Tool (SWAT). An ensemble mean for ten GCMs and three greenhouse gas emissions scenarios (A1B, A2 and B1) was used to create future scenarios to run the calibrated and validated SWAT model.

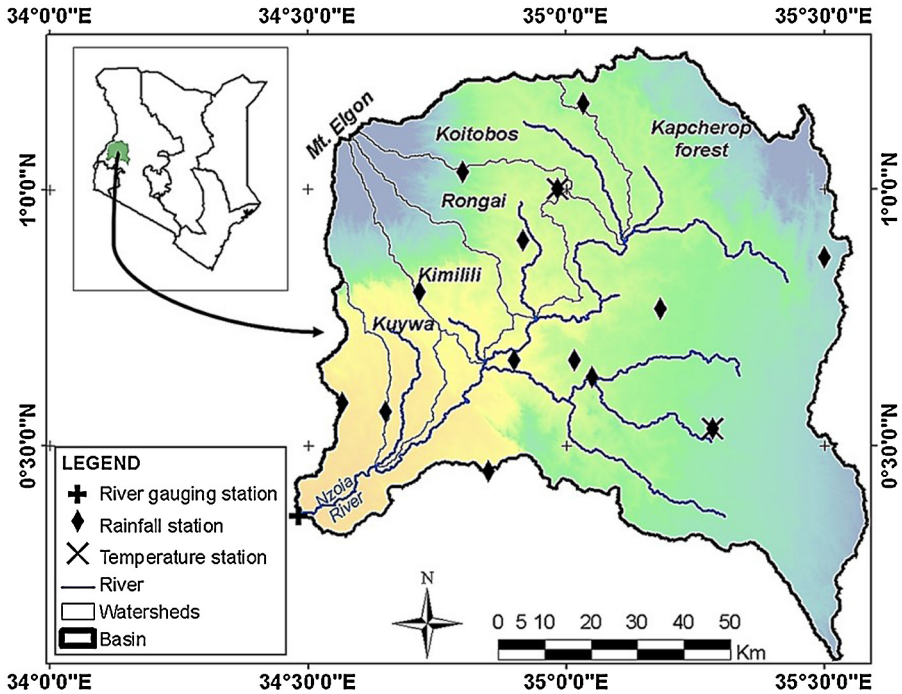


Fig. 1. Location of the study area and hydro-meteorological stations in the Upper Nzoia River basin and its sub basins Kuywa, Kimilili, Rongai and Koitobos.

## 2. Materials and methods

### 2.1. Study area

The study area consists of the upper reaches of the Nzoia River basin (Fig. 1). The river is fed by tributaries flowing from the south-eastern slopes of Mt. Elgon and the Kapcherop forest in western Kenya. It drains to the south-west into Lake Victoria. The catchment area for this study is about 10,156 km<sup>2</sup>, located between longitudes 34.4° and 35.6°E, and latitudes 0.1° and 1.3°N. The area has high topographic relief characterized by steeply sloping uplands and elevation ranging from 878 in the Nzoia River valley to 4304 m a.s.l at the peak of Mt. Elgon. The climate of the area is mainly tropically humid, with mean annual rainfall of 1400–1800 mm and an average temperature of 14–24 °C, though both climate parameters vary strongly with elevation. The annual rainfall pattern is bimodal, with long rains between March and June, and short rains from September to November. Mean temperature is lowest in June to September. Potential evapotranspiration decreases with increasing altitude (Githui et al., 2009). The soils in the area consist of clay, as well as loamy and sandy soil types. In terms of land use, the area is characterized by intensive agricultural activities, forest and significant presence of shrub land. The upper reaches of Mt. Elgon are covered with protected afro-montane forests.

### 2.2. Hydrological modeling

#### 2.2.1. SWAT model

SWAT is a physically based, semi-distributed, basin scale, hydrologic model developed by the United States Department of Agriculture–Agricultural Research Service (USDA–ARS). Its main components are weather conditions, hydrology, soil properties, erosion/sedimentation, plant growth, loads and flows of nutrients, pesticides, bacteria, and pathogens, land management and stream routing (Arnold

**Table 1**  
Global climate models used to generate climate scenarios.

Model	Modeling group (Country)
CGCM3T63	Canadian Center for Climate Modeling and Analysis (Canada)
CNRMCM3	Center National de Recherches Meteorologiques (France)
CSIROMk3.0	Commonwealth Scientific and Industrial Research Organization (Australia)
ECHO-G	University of Bonn, Meteorological Research Institute (Germany)
GISS-ER	Goddard Institute for Space Studies (USA)
MRI CGCM2.3.2	Meteorological Research Institute (Japan)
IPSLCM4	Institut Pierre Simon Laplace (France)
GFDLCM2.1	NOAA Geophysical Fluid Dynamics Lab (United States)
ECHAM5OM	Max Planck Institute for Meteorology (Germany)
HadCM3	Hadley Centre for Climate Prediction and Research (UK)

et al., 1998). In this model, basins are sub-divided into multiple sub-watersheds which are further sub-divided using combinations of soil, land use and slope to form hydrologic response units (HRUs) (Arnold et al., 1998; Bouraoui et al., 2002; Neitsch et al., 2011). The water balance equation (Eq. (1)) is used to simulate the hydrological balance for each HRU (Arnold et al., 1998).

$$SW_t = SW_0 + \sum_{i=1}^t (R_{day} - Q_{surf} - E_a - w_{seep} - Q_{gw})_t \quad (1)$$

where  $SW_t$  (in mm) is the final soil water content,  $SW_0$  (in mm) is the initial soil water content on day  $i$ ,  $t$  (day) is the time,  $R_{day}$  (in mm) is the amount of precipitation on day  $i$ ,  $Q_{surf}$  (in mm) is the amount of surface runoff on day  $i$ ,  $E_a$  (in mm) is the amount of evapotranspiration on day  $i$ ,  $w_{seep}$  (in mm) is the amount of water entering the vadose zone from the soil profile on day  $i$ , and  $Q_{gw}$  (in mm) is the amount of return flow on day  $i$ .

### 2.2.2. Data

The topographic characteristics and spatial distribution of land cover/use and soil types facilitate delineation of the stream network and hydrologic response units in the SWAT model. For this study, a 90 m resolution Digital Elevation Model (DEM) was obtained from the NASA Shuttle Radar Topography Mission (SRTM) (Jarvis et al., 2008). The land cover/use map was obtained from the Joint Research Center (JRC) of the European Commission Global Land Cover 2000 dataset (Mayaux et al., 2003) and reclassified according to SWAT model input requirements. Forests are spread widely in the upper and mid-elevation parts of the area, while cropland is located at mid-elevation and in the lower parts. Daily precipitation, maximum air temperature, minimum air temperature, relative humidity, wind speed and solar radiation data are required to drive the water balance model in SWAT. Information on soils in the area was derived from the Kenya Soil and Terrain database (KENSOTER) (KSS ISRIC, 2007). Daily rainfall data (14 stations), and minimum and maximum temperature data (two stations) were obtained from the Kenya Meteorological Department, while relative humidity, wind speed and solar radiation data were simulated using the weather generator in SWAT. This weather generator was also used to fill in missing rainfall and temperature data.

Temperature and rainfall change data for three future periods, 2011–2040 (2020s), 2041–2070 (2050s) and 2071–2100 (2080s), relative to current climatic conditions, were downscaled using the delta-change approach. This method is stable, robust and simple in generating climate scenarios from a group of global climate models, leading to its wide application in previous studies (Andréasson et al., 2004; Boyer et al., 2010; Merritt et al., 2006; Minville et al., 2008). Table 1 shows the GCMs used in this study. The model data was obtained from the Canadian Climate Change Scenarios (CCCSN) website. The monthly rainfall and mean temperature anomalies were then applied to observed daily data in the SWAT model. Thus, rainfall intensity was perturbed by multiplying observed rainfall with monthly change factors, while temperature was perturbed by adding the prescribed monthly change to the respective monthly baseline conditions to obtain daily perturbation (Bouraoui et al., 2002; Mengistu and Sorteberg, 2012). As stated by Boyer et al. (2010), the biases in the GCMs are assumed constant

**Table 2**  
Parameters selected for SWAT model calibration.

Parameter	Description	Range	
ALPHA_BF	Baseflow alpha factor (days)	0	1
CN2	Initial SCS CN II value	±25%	
SOL_AWC	Available water capacity (mm H <sub>2</sub> O mm soil)	0	1
CH_K2	Effective hydraulic conductivity in main channel (mm/h)	5	130
CH_N	Manning's "n" value for the main channel	0	0.3
GWQMN	Threshold depth of water in the shallow aquifer required for return flow to occur (mm)	0	500
ESCO	Soil evaporation compensation factor	0	1
OV_N	Manning's "n" value for overland flow	0.01	30
SURLAG	Surface runoff lag time (days)	0.05	24
RCHRG_DP	Deep aquifer percolation fraction	0	1
GW_REVAP	Groundwater "revap" coefficient	0.02	2
GW_DELAY	Groundwater delay time (days)	0	90
SOL_K	Saturated hydraulic conductivity (mm/h)	±8%	

in both reference and future periods. The temporal variability (daily to interannual) of the observed climate variables during the reference period is also maintained for the simulated series.

### 2.2.3. SWAT model setup

Based on the DEM, the area was divided into 22 sub-watersheds using the 1DD01A River gauging station (Latitude 0.37° N, Longitude 34.49° E) as the main outlet (Fig. 1). Based on land use, soil type and slope, the sub-watersheds were further divided into a total of 345 hydrologic response units (HRUs). The modified Soil Conservation Service (SCS) curve number method was used to estimate surface runoff from precipitation summed across all the HRUs in a sub-watershed based on soil, land use, and management information (US-Soil Conservation Service Engineering Department, 1972). The Hargreaves method was used for estimating potential evapotranspiration, while channel runoff routing was simulated using the variable storage method (Neitsch et al., 2011).

### 2.2.4. Model calibration and uncertainty analysis

The periods 1986–1998 and 1973–1985 were used for stream flow calibration and validation respectively. A latter period (1986–1998) was selected for model calibration because both the meteorological and streamflow records during this period were complete and they presented both low and high flow conditions. The period was thus suitable for training the model to efficiently depict the hydrological processes in the watersheds. Prior to model calibration, the parameters shown in Table 2 were identified as most sensitive based on a sensitivity analysis procedure in SWAT. These parameters represent the groundwater, soil, runoff, evaporation and channel components of the watershed hydrological process. Prior to the final model calibration, the parameter ranges were modified manually based on correlation between the simulated and observed streamflow while ensuring sufficient parameter space as well as fast convergence. In the manual calibration, the default parameter values for the CN2, ALPHA\_BF, SOL\_AWC, RCHRG\_DP, GW DELAY, SURLAG and SOL\_K were adjusted to improve on the volume and timing of the simulated flow hydrograph. These parameters were selected due to their influence on the runoff and baseflow generation in the SWAT model.

The sequential uncertainty fitting (SUFI-2) algorithm in the SWAT CUP software was used for auto-calibration and uncertainty analysis (Abbaspour et al., 2007). SUFI-2 is a widely used tool for combined calibration and uncertainty analysis of the SWAT model (Faramarzi et al., 2010; Setegn et al., 2008; Strauch et al., 2012). As shown by Yang et al. (2008), SUFI-2 requires fewer simulations compared to the Generalized Likelihood Uncertainty Estimation (GLUE), Parameter Solution (ParaSol), and Bayesian inference techniques to achieve a similar level of performance. In SUFI-2, both relative and absolute parameter ranges were used to generate combinations of parameter values within which optimum values are identified by comparing simulated and observed data (Chien et al., 2013). The fitted parameter sets are drawn independently using Latin hypercube sampling and are expressed in terms of narrowed

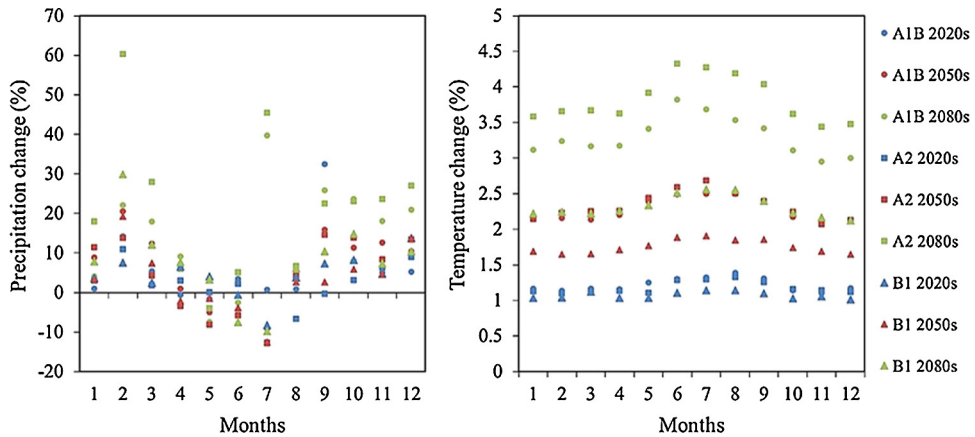


Fig. 2. Ensemble means of projected monthly precipitation and temperature changes by the 2020s, 2050s and 2080s under climate scenarios A1B, A2 and B1.

parameter ranges (Strauch et al., 2012; Yang et al., 2008). The parameter values can be modified either by replacement of the initial value, addition of absolute change or multiplication by a relative change factor to obtain the optimum value. A step-by-step description of the SUFI-2 optimizing algorithm is outlined by Yang et al. (2008).

Model performance was evaluated using the  $p$ -factor,  $r$ -factor, coefficient of determination ( $R^2$ ), and Nash-Sutcliffe efficiency (NSE). The  $p$ -factor represents the percentage of observed data enclosed by the 95% prediction uncertainty (95PPU) whereas the  $r$ -factor is the average width of the 95PPU divided by the standard deviation of the observations. The goal of SUFI-2 is to minimize the width of the uncertainty bound and enclose as many observations as possible (Abbaspour et al., 1997).  $R^2$  values range from 0 to 1, with values greater than 0.5 generally considered acceptable. NSE measures the model efficiency as a fraction of the measured stream flow variance reproduced by the model in replicating individual values. NSE values range between  $-\infty$  and 1, whereby values between 0.36 and 0.75 are considered satisfactory, while values  $\geq 0.75$  are considered excellent (Geza et al., 2009).

### 2.3. Climate change scenarios

The climate change scenarios used in this study represented the minimum and maximum expected precipitation and temperature changes for all the ten climate models used. Fig. 2 shows the ensemble means of projected monthly precipitation and temperature scenarios. The scenarios consisted of monthly percentage change for rainfall (multiplicative factor) and degrees Celsius change for temperature (additive factor) in the future periods relative to the baseline period (1961–1990) for each GCM projection. The relative monthly rainfall variations show a generally unidirectional pattern for the analyzed scenarios and time periods. In the 2020s, under scenario A1B, a major increase in monthly precipitation is projected in February (14.2%) and September (32.5%), while a decrease is expected in April (−0.6%) and May (−1.6%). Under the B1 scenario, the projected mean monthly changes by the 2020s are higher than in the 2050s, but lower compared to the 2080s. The projected increase in April (6.6%) and May (4.0%) for the 2020s, reverses to a negative change in the 2050s (−2.2% and −1.5% for April and May, respectively), and again shows an increase to 7.7% and 3.3% by the 2080s. Unlike the precipitation anomalies, monthly temperature anomalies show a fairly consistent increasing trend irrespective of climate scenario. Projected temperature change ranges between 0.2 and 2.4 °C for the 2020s, 0.9 and 4.0 °C for the 2050s and 1.0 and 5.9 °C for the 2080s depending on the emissions scenario and climate model. All the models indicate that the greatest warming occurs from May to September.



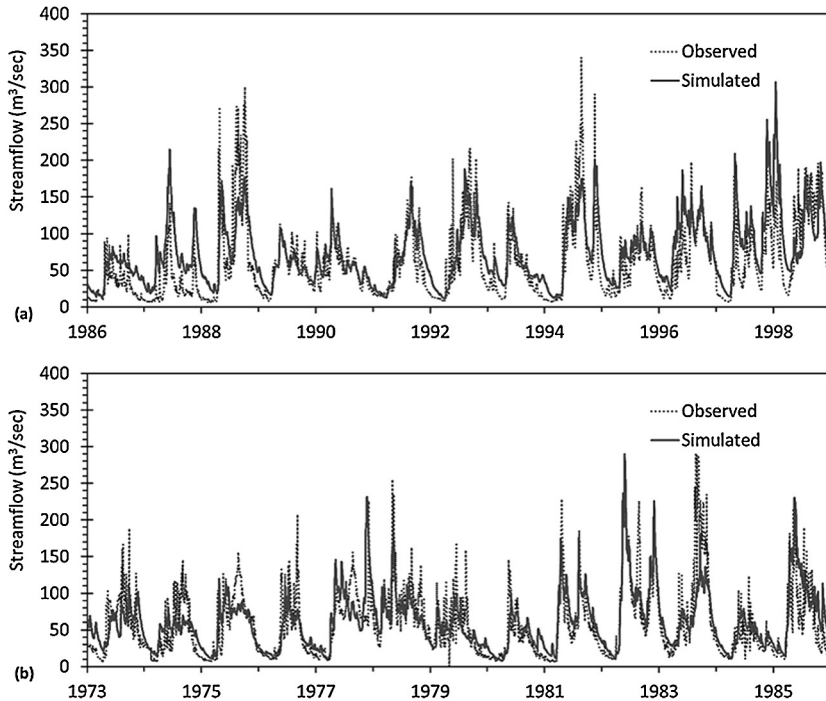


Fig. 3. Daily hydrographs for calibration (a) and validation (b) periods.

### 3. Results and discussion

#### 3.1. SWAT calibration and validation

The sensitivity values from the parameter estimation in SUFI-2 indicated that 6 parameters were highly sensitive: Deep aquifer percolation fraction (RCHRG\_DP), Groundwater “revap” coefficient (GW\_REVAP), soil evaporation compensation factor (ESCO), threshold depth of water in the shallow aquifer for return flow to occur (GWQMN.gw), initial SCS curve number II value (CN2) and groundwater delay time (GW\_DELAY). The 95PPU enclosed 61% of the observed flow data, and an  $r$ -factor of 0.97 was obtained. The optimal parameter combinations simulated the observed flow well in the SWAT model. The  $R^2$  values for daily flow simulation were 0.63 and 0.61, and NSE values were 0.54 and 0.61 for the calibration and validation periods, respectively. The simulated monthly flow also corresponded well with observed flow, with  $R^2$  values of 0.68 and 0.70 and NSE values of 0.58 and 0.70 for the calibration and validation periods, respectively. Fig. 3 shows the daily flow hydrographs for the calibration (1986–1998) and validation (1973–1985) periods.

#### 3.2. Projected streamflow changes

##### 3.2.1. Mean annual streamflow changes

Climate change is likely to cause varied hydrological impacts due to the projected spatial and temporal variation in changes of temperature and precipitation. In this study, hydrological impacts were determined based on averaged anomalies for all climate models per emission scenario and future period. The mean annual streamflow response to the climate scenarios is summarized in Table 3 in terms of the possible decrease and increase. Relative changes in annual mean streamflow exhibited a large uncertainty when the projected temperature and precipitation changes were used in the SWAT model. In the Koitobos watershed, the mean annual flow is projected to change by  $-51.8\%$  to  $73.8\%$

**Table 3**  
Projected annual streamflow changes.

		Koitobos	Rongai	Kimilili	Kuywa
2020s	A1B	[−42.3%, 78.3%]	[−43.3%, 90.2%]	[−40.2%, 83.6%]	[−48.9%, 58.4%]
	A2	[−40.7%, 59.2%]	[−40.9%, 86.1%]	[−37.5%, 81.5%]	[−46.8%, 57.2%]
	B1	[−50.2%, 64.6%]	[−52.7%, 92.9%]	[−51.0%, 86.4%]	[−59.3%, 67.2%]
2050s	A1B	[−49.6%, 93.9%]	[−50.3%, 135.6%]	[−46.3%, 112.4%]	[−56.5%, 85.1%]
	A2	[−51.8%, 73.8%]	[−51.0%, 99.4%]	[−47.8%, 90.4%]	[−59.2%, 66.2%]
	B1	[−39.3%, 58.1%]	[−39.6%, 82.5%]	[−36.9%, 76.3%]	[−51.0%, 51.5%]
2080s	A1B	[−52.7%, 141.5%]	[−51.4%, 185.1%]	[−48.7%, 154.6%]	[−59.6%, 125.2%]
	A2	[−41.8%, 149.4%]	[−42.6%, 189.6%]	[−40.2%, 155.1%]	[−48.8%, 131.6%]
	B1	[−51.5%, 76.2%]	[−51.7%, 107.0%]	[−49.2%, 95.6%]	[−58.3%, 69.0%]

in 2050s and by −41.8% to 149.4% in 2080s under A2 scenario. The annual mean flow in the Rongai watershed is likely to change by between −43.3% and 90.2% by 2020s and −50.2% and 135.6% by 2050s under A1B scenario. In this watershed, by the 2080s under the A2 scenario, the range of expected streamflow change is −42.6% and 189.6%. Under the B1 scenario, mean annual streamflow in Rongai is expected to change by between −52.7% and 92.9% by the 2020s, −39.6% to 82.5% by the 2050s, and −51.7% to 107.0% by the 2080s. The projected change in the mean annual streamflow in Kimilili under

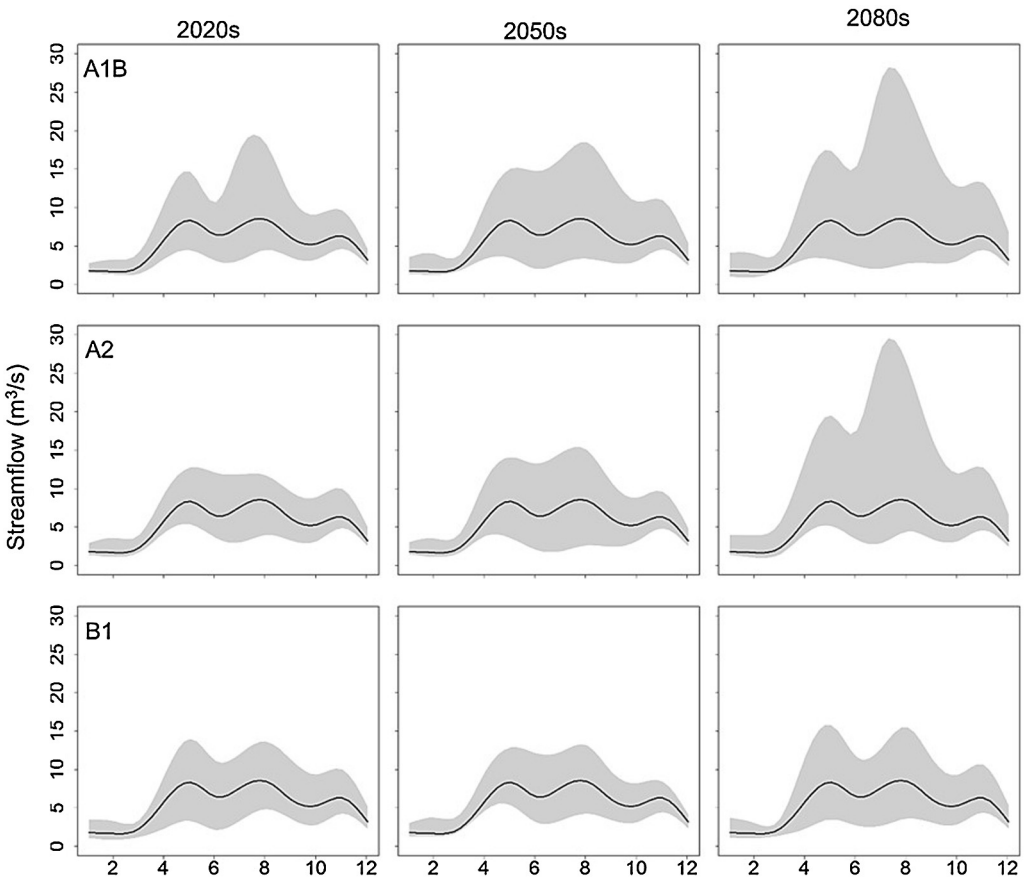


**Fig. 4.** Projected monthly streamflow changes in Koitobos watershed.



scenario A2 is  $-37.5\%$  to  $81.5\%$  and  $-47.8\%$  to  $90.4\%$  for the 2020s and 2050s, respectively, and  $-51.0\%$  to  $51.5\%$  under scenario B1 for the 2050s. In the Kuywa watershed, annual streamflow is expected to change by between  $-59.2\%$  and  $66.2\%$  by 2050 and  $-48.8\%$  and  $131.6\%$  by 2080s under the A2 scenario.

3.2.2. Mean monthly streamflow changes

The projected monthly streamflow changes in the Koitobos watershed are shown in Fig. 4. By the 2020s, under the A1B scenario, streamflow in Koitobos shows a wide uncertainty particularly in March to September. In this period, the projected streamflow shows a likely change by between  $-46.6\%$  and  $75.4\%$  in May and  $-46.4\%$  and  $115.8\%$  in August under the A1B scenario.

For the A2 scenario, in the same period and watershed, a reduced amount of uncertainty in streamflow change is expected. A wide range of expected changes is shown between April and October. In this scenario, the increase in monthly streamflow is likely to reach up to  $59.3\%$  in April, and  $66.8\%$  in October, while the decrease is expected to reach up to  $60.8\%$  in July. The B1 scenario projections for this watershed for the 2020s period show that streamflow has a high uncertainty in April, May and August. By the 2050s, the A1B scenario shows a similar pattern of streamflow change as the 2020s period, but the magnitude of the uncertainty in the projected changes is greater. Scenario A2 also shows a similar pattern, but higher magnitude of changes by the 2050s compared to the 2020s. Scenario B1 in this period projects that flow is likely to change by between  $-15.5\%$  and  $79.0\%$  in March,  $-43.3\%$  and  $86.6\%$  in September,  $-40.4\%$  and  $74.8\%$  in October, and  $-29.0\%$  and  $68.6\%$  in November. By the 2080s, for

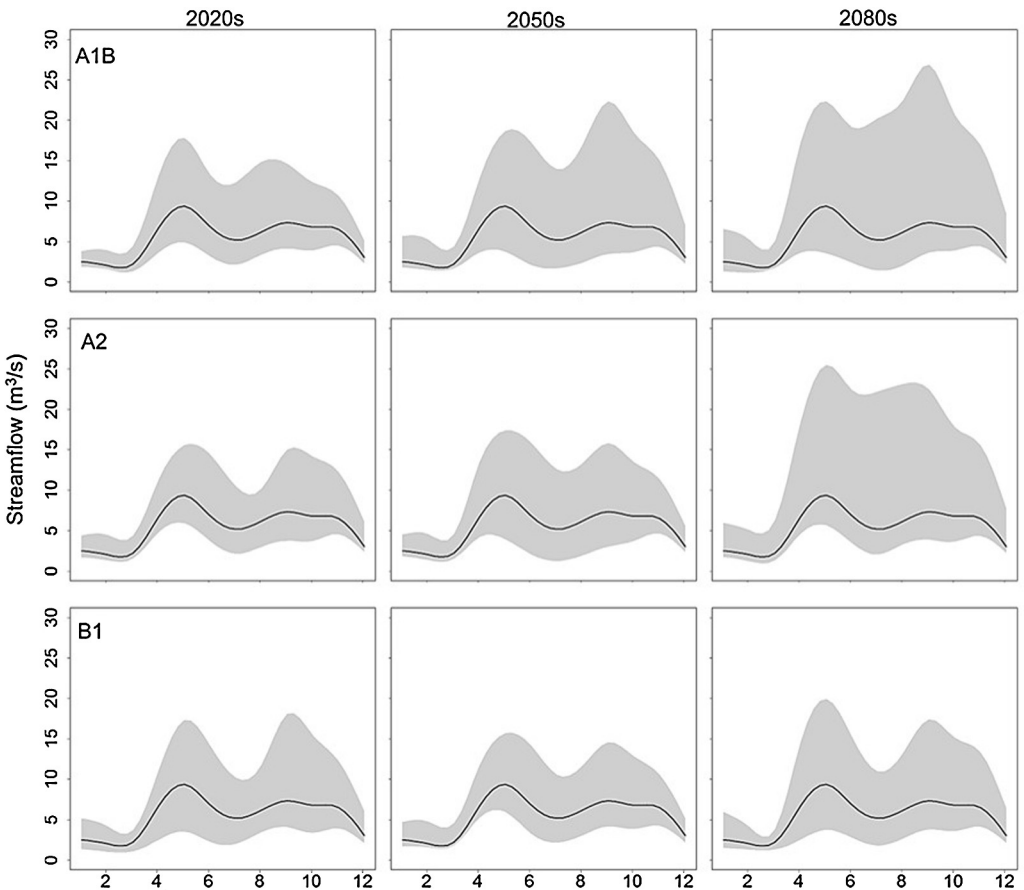


Fig. 5. Projected monthly streamflow changes in Rongai watershed.

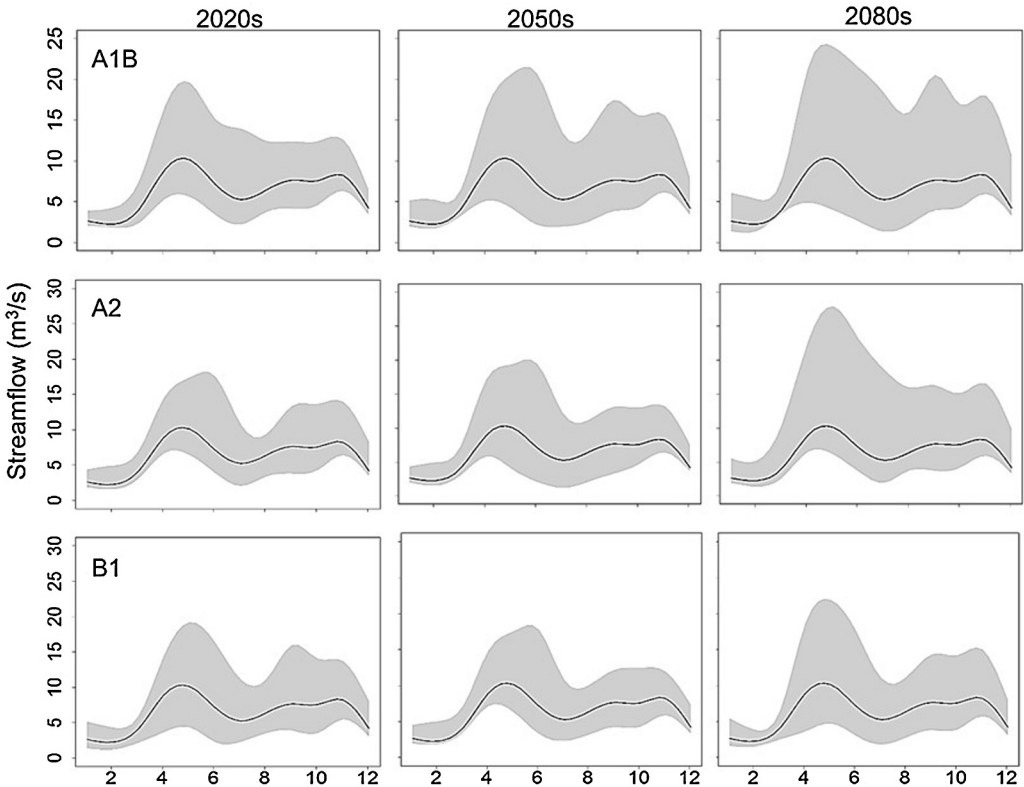


Fig. 6. Projected monthly streamflow changes in Kimilili watershed.

scenario A1B, a similar pattern of change as for the 2050s is expected, except that the uncertainty in the projected flow in June, September and October increases. Streamflow changes of between  $-44.4\%$  and  $125.5\%$  in April and between  $-67.5\%$  and  $201.6\%$  are expected in this period. Under the A2 scenario in the 2080s, flow is expected to change by  $-29.6\%$  to  $138.4\%$  in April,  $-38.4\%$  to  $133.9\%$  in May and  $-48.1\%$  to  $172.4\%$  in June, while under the B2 scenario, a similar pattern of change is expected but with lower uncertainty.

The pattern of streamflow change in Rongai, Kimilili and Kuywa is shown in Figs. 5–7. As shown in Fig. 5, large increases by the 2020s are expected in August to November under all emission scenarios in the Rongai watershed. During this period, large flow decreases are likely to occur in April to July. In the Kimilili watershed, as shown in Fig. 6, by the 2020s scenarios A1B indicates that streamflow in February is likely to change by  $-20.1\%$  to  $90.3\%$ , while in September, flow is likely to change by  $-45.7\%$  to  $62.0\%$ . The Kuywa watershed exhibits similar patterns of projected streamflow changes (Fig. 7).

#### 4. Discussion

The streamflow response to climate change was assessed at sub-basin level based on a single-site calibration of the SWAT model. The streamflow simulated by SWAT for the baseline period is consistent with the observed flow data during the calibration and validation periods. A single site was used for calibration and validation due to lack of reliable data upstream. Consequently, spatial variation in hydrologic responses of sub-basins was not well simulated. Collection of multi-site and multi-variable data is necessary to improve the model calibration (Chien et al., 2013). Spatio-temporal variability in streamflow can be caused by changes in climatic factors as well as land use/cover features

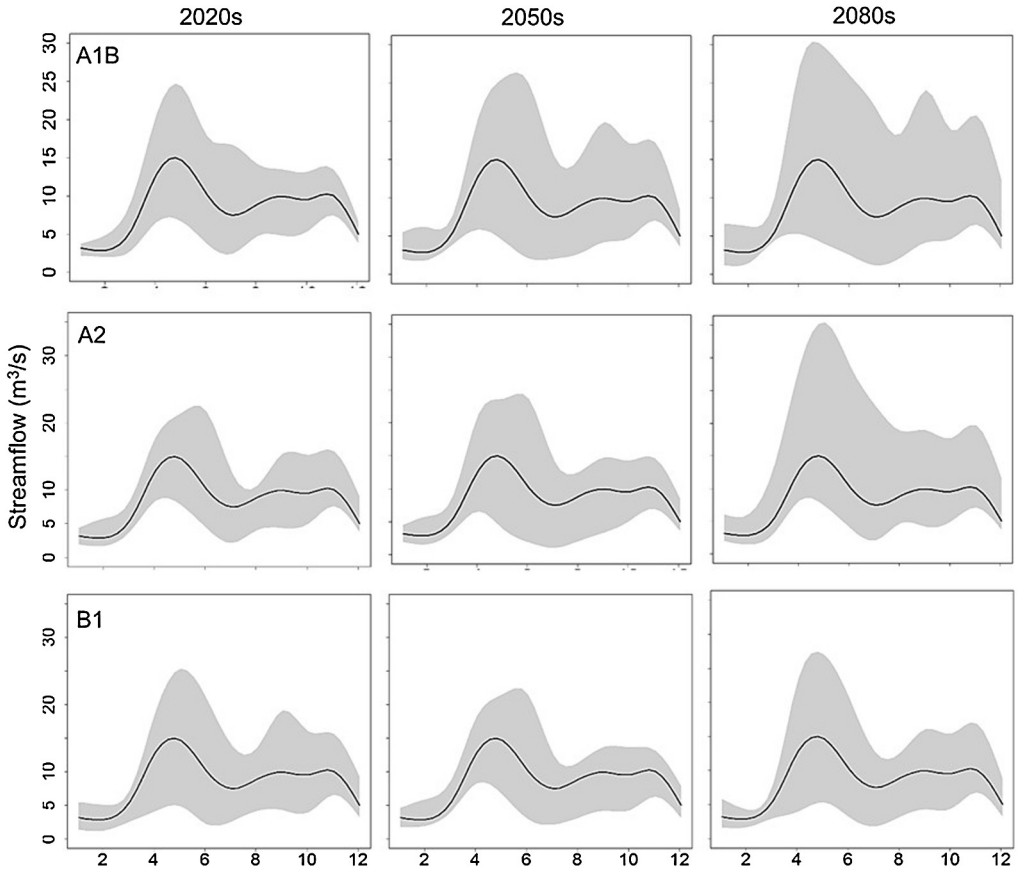


Fig. 7. Projected monthly streamflow changes in Kuywa watershed.

(Kim et al., 2013; Tu, 2009; Wang et al., 2013). The effect of land use/cover change on streamflow was not considered in this study; hence climate change was the primary factor causing the streamflow change.

The study demonstrates diverse streamflow responses in Mt. Elgon watersheds under climate change. Projected monthly streamflow changes vary across the watersheds. The results show that August to December streamflow is likely to be highly altered in the Koitobos and Kimilili watersheds, while in the Kuywa watershed, March to June flows are likely to change considerably due to climate change. In Rongai watershed, major streamflow changes are likely in March to June, and August to November. Streamflow variability in the four watersheds was different, suggesting varied buffering capabilities in response to climate forcing in the four watersheds. The watersheds are characterized by varied coverage of forest and protected area as well as agricultural land use activities which is likely to affect their respective runoff generation mechanisms despite their proximity.

The results of this study are characterized by uncertainties emanating from the GCM projections, the hydrological model and model parameters. The estimation of orographic climate data in SWAT is based on elevation bands as well as the mean difference between the gauging station elevation and mean elevation of each band. The estimated runoff impacts can be improved by use of climatic data with a high spatial resolution to account for spatial variation in climatic parameters. Calibrated SWAT model parameters were assumed to remain constant in future climatic conditions. Spatial and temporal generalization of results will, therefore, require consideration of the spatial-temporal patterns of

climate as well as change in land use patterns due to human activities to better capture uncertainties in hydrological responses.

Climate change impact was assessed based on relative monthly anomalies of rainfall and temperature. The downscaling approach used in this study assumes that rainfall frequency in the baseline period remains similar across future periods. We, therefore, recommend that a more advanced downscaling method be used, as different downscaling methods may produce different future climate projections.

## 5. Conclusions

In this study, the potential implications of climate change for streamflow in the upper Nzoia River basin were assessed using the SWAT model. The model was calibrated and validated over the 1986–1998 and 1973–1985 periods, respectively. The SWAT model efficiently captured the historical hydrological processes in the upper Nzoia Basin based on the observed meteorological data. Thus, this model can be applied in understanding of the dynamic water balance processes in this area.

The delta change downscaling method was used to generate three scenarios of projected changes in future rainfall and temperature for each of three future time periods: the 2020s (2011–2030), the 2050s (2041–2070) and the 2080s (2071–2100). The baseline and future periods were compared in terms of relative change. Large uncertainties in the future precipitation, temperature and streamflow are expected. At sub-basin level, the streamflow response to precipitation and temperature change is nonlinear. However, projected streamflow changes are highly dependent on the direction of projected precipitation changes, as concluded also by [Shrestha et al. \(2013\)](#) and [Kingston et al. \(2011\)](#). Sub-basins showed distinct responses despite their proximity which the authors attribute to differences in land use activities and soil types. In the four watersheds, projected streamflow change shows high uncertainty during the wet period (April to June and August to November). The quantitative impacts of these changes will have significant implications for development and ecosystems in the watersheds and downstream areas.

This study provides a wide range of expected changes in streamflow, basic climatic characteristics and the associated uncertainty. Despite the uncertainty in the projections, the study presents useful insights for long-term basin-wide strategic planning and implementation of development projects, disaster preparedness strategies and water resources management in this important basin. The projections show likely high increases of streamflow, particularly between August and November, which ought to sound an alarm for reassessment of the design and sustainability of flood and landslide disaster management and mitigation measures in the area. The significance of a multi-model approach in climate change impact assessment has also been highlighted. The use of multi-climate models to force different hydrological models would provide a detailed picture of expected uncertainties, as well as possible hydrological responses and trends in the basin. Consequently, we recommend a well-coordinated hydrological impact assessment in the region, based on regionally downscaled climate projections to clearly expose what is certain and what is uncertain about expected changes to regional-scale hydrology in the Mt. Elgon area.

## Conflict of interest

No conflict of interest.

## Acknowledgement

We are grateful to The Rockefeller Foundation for supporting this work under the umbrella of the project “AdaptEA–Adaptation of People to Climate Change in East Africa: Forest Ecosystem services, Risk Reduction and Human Well-being” (led by the Center for International Forestry Research), under grant no. 2011 CRD 306. We also acknowledge support from the CGIAR Collaborative Research Programs on Water, Land and Ecosystems (WLE), as well as Climate Change, Agriculture and Food Security (CCAFS).

## References

- Abbaspour, K.C., van Genuchten, M.T., Schulin, R., Schläppi, E., 1997. A sequential uncertainty domain inverse procedure for estimating subsurface flow and transport parameters. *Water Resour. Res.* 33, 1879–1892, <http://dx.doi.org/10.1029/97WR01230>.
- Abbaspour, K.C., Yang, J., Maximov, I., Siber, R., Bogner, K., Mieleitner, J., Zobrist, J., Srinivasan, R., 2007. Modelling hydrology and water quality in the pre-alpine/alpine Thur watershed using SWAT. *J. Hydrol.* 333, 413–430, <http://dx.doi.org/10.1016/j.jhydrol.2006.09.014>.
- Andréasson, J., Bergström, S., Carlsson, B., Graham, L.P., Lindström, G., 2004. Hydrological change – climate change impact simulations for Sweden. *AMBIO A J. Hum. Environ.* 33, 228–234, <http://dx.doi.org/10.1579/0044-7447-33.4.228>.
- Arnell, N.W., 2011. Uncertainty in the relationship between climate forcing and hydrological response in UK catchments. *Hydrol. Earth Syst. Sci.* 15, 897–912, <http://dx.doi.org/10.5194/hess-15-897-2011>.
- Arnold, J., Srinivasan, R., Mutiiah, R., Williams, J., 1998. *Large-area hydrologic modeling and assessment. Part I: model development.* *J. Am. Water Resour. Assoc.* 34, 73–89.
- Bastola, S., Murphy, C., Sweeney, J., 2011. The role of hydrological modelling uncertainties in climate change impact assessments of Irish river catchments. *Adv. Water Resour.* 34, 562–576, <http://dx.doi.org/10.1016/j.advwatres.2011.01.008>.
- Bates, B.C., Kundzewicz, Z.W., Wu, S., Palutikof, J.P., 2008. *Climate change and water. Technical Paper. Intergovernmental Panel on Climate Change, Geneva.*
- Bourauoi, F., Galbiati, L., Bidoglio, G., 2002. Climate change impacts on nutrient loads in the Yorkshire Ouse catchment (UK). *Hydrol. Earth Syst. Sci.* 6, 197–209, <http://dx.doi.org/10.5194/hess-6-197-2002>.
- Boyer, C., Chaumont, D., Chartier, I., Roy, A.G., 2010. Impact of climate change on the hydrology of St. Lawrence tributaries. *J. Hydrol.* 384, 65–83, <http://dx.doi.org/10.1016/j.jhydrol.2010.01.011>.
- Braga, A.C.F.M., Silva, R.M.Da., Santos, C.A.G., Galvão, C.D.O., Nobre, P., 2013. Downscaling of a global climate model for estimation of runoff, sediment yield and dam storage: a case study of Pirapama basin, Brazil. *J. Hydrol.* 498, 46–58, <http://dx.doi.org/10.1016/j.jhydrol.2013.06.007>.
- Brigode, P., Oudin, L., Perrin, C., 2013. Hydrological model parameter instability: a source of additional uncertainty in estimating the hydrological impacts of climate change? *J. Hydrol.* 476, 410–425, <http://dx.doi.org/10.1016/j.jhydrol.2012.11.012>.
- Chen, J., Brissette, F.P., Leconte, R., 2011. Uncertainty of downscaling method in quantifying the impact of climate change on hydrology. *J. Hydrol.* 401, 190–202, <http://dx.doi.org/10.1016/j.jhydrol.2011.02.020>.
- Chien, H., Yeh, P.J.-F., Knouft, J.H., 2013. Modeling the potential impacts of climate change on streamflow in agricultural watersheds of the Midwestern United States. *J. Hydrol.* 491, 73–88, <http://dx.doi.org/10.1016/j.jhydrol.2013.03.026>.
- Chiew, F., Kirono, D., Kent, D., Frost, A., Charles, S., Timbal, B., Nguyen, K., Fu, G., 2010. Comparison of runoff modelled using rainfall from different downscaling methods for historical and future climates. *J. Hydrol.* 387, 10–23, <http://dx.doi.org/10.1016/j.jhydrol.2010.03.025>.
- Claessens, L., Knäpen, A., Kitutu, M.G., Poesen, J., Deckers, J.A., 2007. Modelling landslide hazard, soil redistribution and sediment yield of landslides on the Ugandan footslopes of Mount Elgon. *Geomorphology* 90, 23–35, <http://dx.doi.org/10.1016/j.geomorph.2007.01.007>.
- Faramarzi, M., Yang, H., Schulin, R., Abbaspour, K.C., 2010. Modeling wheat yield and crop water productivity in Iran: implications of agricultural water management for wheat production. *Agric. Water Manage.* 97, 1861–1875, <http://dx.doi.org/10.1016/j.agwat.2010.07.002>.
- Ficklin, D., Luo, Y., Luedeling, E., Zhang, M., 2009. Climate change sensitivity assessment of a highly agricultural watershed using SWAT. *J. Hydrol.* 374, 16–29, <http://dx.doi.org/10.1016/j.jhydrol.2009.05.016>.
- Geza, M., Poeter, E.P., McCray, J.E., 2009. Quantifying predictive uncertainty for a mountain-watershed model. *J. Hydrol.* 376, 170–181, <http://dx.doi.org/10.1016/j.jhydrol.2009.07.025>.
- Githui, F., Gitau, W., Bauwens, W., 2009. Climate change impact on SWAT simulated streamflow in western Kenya. *J. Clim.* 29, 1823–1834, <http://dx.doi.org/10.1002/joc.1828>.
- Hagg, W., Braun, L.N., Kuhn, M., Nesgaard, T.I., 2007. Modelling of hydrological response to climate change in glacierized Central Asian catchments. *J. Hydrol.* 332, 40–53, <http://dx.doi.org/10.1016/j.jhydrol.2006.06.021>.
- Hansen, J., Sato, M., Ruedy, R., Lo, K., Lea, D., Medina-Elizade, M., 2006. Global temperature change-European Environment Agency (EEA). *Proc. Natl. Acad. Sci. U. S. A.* 103, 14288–14293, <http://dx.doi.org/10.1073/pnas.0606291103>.
- IPCC, 2007. *Summary for policymakers.* In: Solomon, S., Qin, D., Manning, M., Chen, Z., Marquis, M., Averyt, K.B., Ignor, M.T., Miller, H.L. (Eds.), *Contribution of Working Group I to the Fourth Assessment Report of the Intergovernmental Panel on Climate Change, 2007.* Cambridge University Press, Cambridge, United Kingdom and New York, NY, USA.
- Jarvis, A., Reuter, H.L., Nelson, A., Guevara, E., 2008. Hole-filled SRTM for the globe Version 4, Available from the CGIAR-CSI SRTM 90m Database (<http://srtm.csi.cgiar.org>).
- Kay, A.L., Jones, R.G., Reynard, N.S., 2006. RCM rainfall for UK flood frequency estimation, II. Climate change results. *J. Hydrol.* 318, 163–172, <http://dx.doi.org/10.1016/j.jhydrol.2005.06.013>.
- Kim, J., Choi, J., Choi, C., Park, S., 2013. Impacts of changes in climate and land use/land cover under IPCC RCP scenarios on streamflow in the Hoya River Basin. *Kor. Sci. Total Environ.* 452–453, 181–195, <http://dx.doi.org/10.1016/j.scitotenv.2013.02.005>.
- Kingston, D.G., Taylor, R.G., 2010. Sources of uncertainty in climate change impacts on river discharge and groundwater in a headwater catchment of the Upper Nile Basin. *Uganda Hydrol. Earth Syst. Sci.* 14, 1297–1308, <http://dx.doi.org/10.5194/hess-14-1297-2010>.
- Kingston, D.G., Thompson, J.R., Kite, G., 2011. Uncertainty in climate change projections of discharge for the Mekong River Basin. *Hydrol. Earth Syst. Sci.* 15, 1459–1471, <http://dx.doi.org/10.5194/hess-15-1459-2011>.
- KSS, ISRIC, 2007. Kenya Soil and Terrain database at scale 1:1,000,000 – version 2. Kenya Soil Survey and ISRIC-World Soil Information, <http://www.isric.org/data/soil-and-terrain-database-kenya-primary-data>
- Liu, X., Coulibaly, P., Evora, N., 2008. Comparison of data-driven methods for downscaling ensemble weather forecasts. *Hydrol. Earth Syst. Sci.* 12, 615–624.
- Matondo, J.I., Peter, G., Msibi, K.M., 2004. Evaluation of the impact of climate change on hydrology and water resources in Swaziland: Part II. *Phys. Chem. Earth* 29, 1193–1202, <http://dx.doi.org/10.1016/j.pce.2004.09.035>.

- Mayaux, P., Massart, M., Cutsem, C. Van, Cabral, A., Nonguierma, A., Diallo, O., Pretorius, C., Thompson, M., Cherlet, M., Defourny, P., Vasconcelos, M., Gregorio, A. Di, Grandi, G. De, Belward, A., 2003. *GLC 2000: A land cover map of Africa*.
- Mengistu, D.T., Sorteberg, A., 2012. Sensitivity of SWAT simulated streamflow to climatic changes within the Eastern Nile River basin. *Hydrol. Earth Syst. Sci.* 16, 391–407, <http://dx.doi.org/10.5194/hess-16-391-2012>.
- Merritt, W.S., Alila, Y., Barton, M., Taylor, B., Cohen, S., Neilsen, D., 2006. Hydrologic response to scenarios of climate change in sub watersheds of the Okanagan basin, British Columbia. *J. Hydrol.* 326, 79–108, <http://dx.doi.org/10.1016/j.jhydrol.2005.10.025>.
- Minville, M., Brissette, F., Leconte, R., 2008. Uncertainty of the impact of climate change on the hydrology of a nordic watershed. *J. Hydrol.* 358, 70–83, <http://dx.doi.org/10.1016/j.jhydrol.2008.05.033>.
- Murphy, J., 1998. An evaluation of statistical and dynamical techniques for downscaling local climate. *J. Clim.* 12, 2256–2284.
- Neitsch, S.L., Arnold, J.G., Kiniry, J.R., Williams, J.R., 2011. *Soil & Water Assessment Tool Theoretical Documentation Version 2009. Texas Water Resources Institute Technical Report No. 406*.
- Peterson, J.G., Kaboggoza, J., 2006. *Transboundary biodiversity management challenges; the case of Mt. Elgon, Uganda and Kenya*.
- Setegn, S.G., Srinivasan, R., Dargahi, B., 2008. *Hydrological modelling in the Lake Tana Basin, Ethiopia using SWAT model*. *Open Hydrol. J.* 2008, 49–62.
- Shrestha, B., Babel, M.S., Maskey, S., van Griensven, A., Uhlenbrook, S., Green, A., Akkharath, I., 2013. Impact of climate change on sediment yield in the Mekong River basin: a case study of the Nam Ou basin, Lao PDR. *Hydrol. Earth Syst. Sci.* 17, 1–20, <http://dx.doi.org/10.5194/hess-17-1-2013>.
- Strauch, M., Bernhofer, C., Koide, S., Volk, M., Lorz, C., Makeschin, F., 2012. Using precipitation data ensemble for uncertainty analysis in SWAT streamflow simulation. *J. Hydrol.* 414–415, 413–424, <http://dx.doi.org/10.1016/j.jhydrol.2011.11.014>.
- Teng, J., Vaze, J., Chiew, F.H.S., Wang, B., Perraud, J.-M., 2012. Estimating the relative uncertainties sourced from GCMs and hydrological models in modeling climate change impact on runoff. *J. Hydrometeorol.* 13, 122–139, <http://dx.doi.org/10.1175/JHM-D-11-058.1>.
- Tu, J., 2009. Combined impact of climate and land use changes on streamflow and water quality in eastern Massachusetts, USA. *J. Hydrol.* 379, 268–283, <http://dx.doi.org/10.1016/j.jhydrol.2009.10.009>.
- US-Soil Conservation Service Engineering Department, 1972. *Section 4: Hydrology, in: National Engineering Handbook*.
- Wang, S., Zhang, Z.R., McVicar, T., Guo, J., Tang, Y., Yao, A., 2013. Isolating the impacts of climate change and land use change on decadal streamflow variation: assessing three complementary approaches. *J. Hydrol.* 507, 63–74, <http://dx.doi.org/10.1016/j.jhydrol.2013.10.018>.
- Wilby, R., Wigley, T., 1998. Downscaling general circulation model output: a review of methods and limitations. *Prog. Phys. Geo.* 21, 530–548.
- Xu, C., 1999. *From GCMs to river flow: a review of downscaling methods and hydrologic modelling approaches*. *Prog. Phys. Geo.* 23, 229–249.
- Xu, H., Taylor, R.G., Xu, Y., 2011. Quantifying uncertainty in the impacts of climate change on river discharge in sub-catchments of the Yangtze and Yellow River Basins, China. *Hydrol. Earth Syst. Sci.* 15, 333–344, <http://dx.doi.org/10.5194/hess-15-333-2011>.
- Xu, Y.-P., Zhang, X., Ran, Q., Tian, Y., 2013. Impact of climate change on hydrology of upper reaches of Qiantang River Basin, East China. *J. Hydrol.* 483, 51–60, <http://dx.doi.org/10.1016/j.jhydrol.2013.01.004>.
- Yang, J., Reichert, P., Abbaspour, K.C., Xia, J., Yang, H., 2008. Comparing uncertainty analysis techniques for a SWAT application to the Chaohu Basin in China. *J. Hydrol.* 358, 1–23, <http://dx.doi.org/10.1016/j.jhydrol.2008.05.012>.